***Supporting Online Material:***

## Materials and Methods

**Strain construction:** The CI-YFP fusion protein (Fig. 1B) was constructed by PCR, and contained the entire coding sequence of the wild-type *cI* gene fused directly to the coding sequence of the *yfp* gene (from pDH5 plasmid, University of Washington Yeast Resource Center). The *cI-yfp* gene was expressed from the tightly regulated $P_{LtetO-1}$ promoter on the pZS21 plasmid (*1*), which is stable and difficult to cure. Integration of CFP with the $P_R$ promoter was performed as previously described (*2*). Since the *cfp* gene is chromosomally integrated, and the repressor concentration is independently measured, the results are not affected by possible variations in plasmid copy number or plasmid loss after the end of induction of *cI-yfp* expression. Full induction of *cI-yfp* expression by anhydrotetracycline (aTc) was sufficient to repress CFP production in the λ-cascade strain to undetectable levels. When not induced, the *cI-yfp* plasmid had no effect on CFP expression. Thus, the strain allows exploration of the full dynamic range of CFP regulation.

The $O_R2$*-λ-cascade strain (Fig. S3) was constructed by site-directed mutagenesis of the $P_R$ promoter (Stratagene QuikChange Kit) with the following primers:

5′-GGATAAATATCTAACACCGTGC**T**TGTTGACTATTTTACCTCTGG and
5′-CCAGAGGTAAAATAGTCAACA**A**GCACGGTGTTAGATAT-TTATCC.

This created a mutation which was previously designated as 'VN' (*3*). The underlined portion of the primers represents $O_R2$ and the bold nucleotide is the site of the point mutation that changes a G to a T. The 'symmetric branch' strain (Fig. 4D) was strain MRR containing plasmid pZS21-cIYFP-Y66F. MRR contains CFP and YFP at separate, but equivalent, loci, approximately equidistant from the origin of replication, each under wild-type $P_R$ promoters (*2*). Plasmid pZS21-cIYFP-Y66F was identical to pZS21-cIYFP, except that site-directed mutagenesis was used to introduce a single point mutation converting the tyrosine at YFP position 66 (in the YFP chromophore) to phenyalanine, thereby eliminating repressor fluorescence.

**Experimental procedure and image acquisition:** Cultures were grown overnight in LB + 15 μg/mL kanamycin at 37°C from single colonies, and diluted 1:100 in MSC media (M9 minimal medium + 0.6% succinate + 0.01% casamino acids + 0.15 μg/ml biotin + 1.5 μM thiamine). Cultures were grown to $OD_{600}$ ~0.1 at 32°C, and then induced if necessary. Induction consisted of adding aTc to a final concentration of 100 ng/mL for ~3 minutes at ambient temperature, followed by 2 washes with MSC to remove aTc (Fig. 1C). Cells were allowed to grow until just prior to the production of the CI-repressed gene(s), then diluted to give ~1 cell per visual field when placed between a coverslip and 1.5% low melt MSC agarose. Growth of microcolonies was observed by fluorescence microscopy at 32ºC using a Leica DMIRB/E automated fluorescence microscope (Fig. 1D and Fig. S1). Cell-cycle period (doubling time) was 45±10min for all strains. Custom Visual Basic software was written to control the microscope and related equipment (Ludl motorized stage and Hamamatsu Orca II CCD camera), via ImagePro Plus and ScopePro packages (Media Cybernetics). In most cases, multiple fields of view were recorded simultaneously (in a loop). Typical intervals between subsequent exposures were 8~9 minutes. In the lambda-cascade strains, YFP fluorescence images were acquired only on alternate frames to reduce photo-bleaching. In the symmetric branch strains, YFP images were taken every frame.

Cellular fluorescence values at time intervals when no CFP or CI-YFP molecules are produced (Fig. 2A) are consistent with negligible rates of protein degradation and photo-bleaching. This was confirmed by separate series of control experiments (data not shown). CI-YFP levels were diluted by cell growth (*4*) (see also 'Math primer', in downloadable data at http://www.weizmann.ac.il/mcb/UriAlon).

**Image analysis and data acquisition:** Custom software was developed using MATLAB (The Mathworks, Inc.) to analyze time-lapse movie data. Analysis proceeds in several stages: First, segmentation of the microcolony was automatically performed on phase-contrast images (Fig. 1D, Fig. S1 and Fig. S4). The quality of the segmentation was checked interactively for each frame and poorly segmented cells were corrected or discarded. A custom tracking algorithm was then applied to the time series of segmented images to obtain a time course for each cell and its descendant lineages. This tracking analysis was also checked manually. Together, these procedures resulted in a lineage tree of the microcolony (Fig. S2) containing fluorescence information at each time-point (Fig. 2A).

Background and cellular auto-fluorescence values were subtracted from each channel and crosstalk from the cyan channel into the yellow channel was corrected for. The segmented image was used to collect the data from the fluorescence images, and the area of each cell at each time point was recorded as the number of pixels in the segmented cell region. The sum of the fluorescence intensity of these pixels was recorded in cyan (C) and yellow (Y) fluorescence channels (Fig 2A). In addition, the cell length (*l*, typical values are 3~4 microns) and width (*w*, narrowly distributed around 0.75 microns) were recorded, and cell volume calculated by modeling the cell as a cigar-shape cylinder of length (l-w) and radius (w/2), capped by two hemispheres of radius (w/2). Cell volumes typically varied from 1~2 $\mu m^3$ to 2~3 $\mu m^3$.

**Calibration by binomial errors in protein partitioning:** In cell division events, a difference is observed between the fluorescence levels of the two daughter cells (Fig. 2A). We measured the total fluorescence of each of the two daughters after division, rescaled them to units of apparent number of molecules (see below), and calculated their sum and their difference (Fig. 2B). We compared the measured differences between the two daughter cells with a random, binomially generated daughter set. This set was sampled using an even binomial distribution from the measured sum of the two daughters. A Kolmogorov-Smirnov test implied that the daughter distribution was consistent with the binomial virtual daughter set, with a significance level of 80%. Thus, fluorescence partitioning during cell division appears binomial. According to the binomial model, the average number of particles received by each daughter (denoted by $N_1$ and $N_2$, such that $N_1+N_2=N_{tot}$) is half the number of particles in the parent, $\langle N_1 \rangle = N_{tot}/2$, and their standard deviation is $\sigma_D \equiv \sqrt{\left\langle \left( N_1 - \frac{N_{tot}}{2} \right)^2 \right\rangle} = \sqrt{N_{tot}}/2$. To a first approximation, we assume that all repressors occur in the cells as dimers, since cI is expected to dimerize in the range of concentrations used for induction (*5*) with a dissociation constant of ~10nM (*6, 7*). Let $v_y$ denote the CI-YFP fluorescence intensity reading given by one CI-YFP dimer in a cell, such that the measured fluorescence value is $Y_1=v_y \cdot N_1$. We expect that

$$\sqrt{\left\langle\left(\frac{Y_1-Y_2}{2}\right)^2\right\rangle}=\sqrt{\left\langle\left(Y_1-\frac{Y_1+Y_2}{2}\right)^2\right\rangle}=\sqrt{\left\langle\left(v_y\cdot N_1-\frac{v_y\cdot N_{tot}}{2}\right)^2\right\rangle}=v_y\cdot\sqrt{\left\langle\left(N_1-\frac{N_{tot}}{2}\right)^2\right\rangle}\equiv v_y\cdot\sigma_D$$

and using the result for $\sigma_D$ gives $\sqrt{\left\langle\left(\frac{Y_1-Y_2}{2}\right)^2\right\rangle}=v_y\cdot\sigma_D=v_y\cdot\sqrt{N_{tot}}\Big/2=\sqrt{v_y}\cdot\frac{\sqrt{Y_1+Y_2}}{2}$.

We grouped the individual division events according to total fluorescence (using an equal number of data points per bin), and calculated, for each group, the RMS difference in fluorescence between two daughters (Fig. 2B). We fit these points to $\sqrt{v_y}\cdot\frac{\sqrt{Y_1+Y_2}}{2}$ with the single free parameter $v_y$, and so could convert the data to $N_1$ and $N_2$. Our results strongly suggest that the fluorescent units do indeed distribute according to a binomial distribution (Fig. 2B), although for larger numbers of molecules the standard deviation grows faster than a square root. This discrepancy may be due to multimerization into octamers (*8*) and larger aggregates, as well as other sources of measurement error, which would be expected to grow linearly. Apparent fluorescence of a CI-YFP monomer is found by dividing $v_y$ by 2. A strain that produces CFP and YFP from identical promoters (*2*) was used to find $v_c$, the in vivo fluorescence of one CFP molecule. The values of $v_y$ and $v_c$ determined in this way were used to calibrate the amount of CI-YFP and of CFP in apparent numbers per cell, and thus to calculate the concentration of repressor in the cells in molar units and the production rates in molecules per minute. Errors in this calibration procedure are expected to originate from measurement errors (which are expected to grow linearly), uneven cellular divisions (in which the septum is off-center), and CI-YFP dimerization/multimerization. A more elaborate inference approach, which will be described elsewhere, results in a $v_y$ of the same order. Different estimates of $v_y$ agree to within a factor 2. Actual numbers of CFP and CI-YFP molecules may differ systematically from the apparent numbers, without affecting their ratios.

**Measurement accuracy and errors**: Possible measurement errors in quantification of cellular fluorescence include errors in segmentation of the images and in calibration of the background and auto-fluorescence values. For each of these steps we compared several alternate quantification or calibration methods and assumptions. We found that the segmentation errors can contribute a relative error of a few percent, and calibration errors can contribute a systematic additive error on the order of 10 molecules per cell (of either CFP or YFP). These errors are demonstrated in Fig. 3B (black). The standard error in estimating the mean GRF is smaller than the marker size in Fig. 3A. The Hill function parameters were calculated separately for each alternate combination of methods. The error margins in Table 1 show the variation in these calculated values.

**Calculating production rates:** To measure the average CFP production rate between movie frames, we took the difference in total CFP level between consecutive time points and divided by their separating time interval (8~9 minutes).

**Dependence on microenvironment:** Growth in a microcolony is a complex process, in which cells are in contact with one another, may experience different local environments over time, and have been observed to generate complex patterns (*9*). We analyzed a movie in which three cells, containing different initial amounts of repressor, were grown simultaneously in the same field of

view (Fig. S5A). The descendants of each initial cell increased CFP expression at different times, corresponding to different densities and to different stages of microcolony development. GRFs obtained from the descendants of each initial cell could be superimposed (Fig. S5B). Thus, the measured GRF appears to be robust to possible differences in growth environments within and between these microcolonies. It will be interesting to see whether other promoters may be specifically regulated by the local micro-environment of the cell.

**Correction for cell-cycle phase:** Normalizing the production rate by the size of the cell did not reduce the spread of points for a given CI-YFP concentration (Fig. 3B), and a similar spread of data points was obtained by plotting the production rate of CFP versus either the total amount per cell or the concentration of CI-YFP. However, the production rate spread was reduced by accounting for the 'age' of the cell. For each cell we defined φ, the 'phase' in the cell-cycle, to be a number growing linearly in time from 0 at the cell's birth until 1 at the time of the cell's division. In exponential growth, the average number of copies, *G,* of any gene starts at *M* for a newly divided cell and grows to *2M,* on average, for a cell about to divide (similar to Fig. 4B). We compared the production rates of 'young' cells ($\varphi<0.15$) to the production rate of 'old' cells ($\varphi>0.85$), and found that the spread of points for the 'old' cells coincides with the spread of points for the 'young' cells shifted by a factor of two in production rate, i.e. for the same concentration of CI-YFP, the 'old' cells produce twice as much CFP as the 'young' cells. The simple assumption that $G=M\cdot(1+\varphi)$, consistent with continuous DNA replication where a gene does not replicate at a specific phase in the cell-cycle, substantially reduced the spread in production rates. We used this method to normalize all production rates (shown in Fig. 3) to $\varphi=0.5$.

**Measuring repression-cooperativity without fluorescent protein fusions:** The regulator dilution method results in an average reduction in regulatory protein concentration of two-fold at each division event. We re-analyzed the microcolony data ignoring the YFP fluorescence and assuming that the ('unknown') repressor were partitioned by half at each cell division event. Analyzed this way, the resulting values of *n* were within 10% of our previously measured values. Thus, the mean cooperativity (*n*) of any stable transcriptional regulatory protein can be obtained without fusing it to a fluorescent protein.

**Autocorrelation time of production rates:** For each cell at each time point in the λ-cascade movies we calculated its production rate rank, compared to other cells with similar repressor concentration (or level, see below). For each pair of time points along a certain lineage (i.e. for one cell and all its ancestors), we recorded the rank at the early and the late time points and the time difference. We then calculated the average autocorrelation of the rankings as a function of the time difference *t* (Fig. 4E). Consistent results were obtained when ranking by bins with constant number of points or with constant repressor ranges, with different data subsets, and when using different quantification parameters, such as binning by repressor concentration or by repressor level. The autocorrelation function C(t), normalized to C(0)=1 at t=0, can be fit by a sum of two exponentials, $C(t)=A_1\cdot 2^{-t/\tau_1}+A_2\cdot 2^{-t/\tau_2}$, with $A_1$~0.65, $\tau_1$~40 min, $A_2$~0.35, and $\tau_2$<5 min. This finding agrees with simulation results for a process with two sources of noise, one rapid and the other slow. Filtering out the rapid component in the production rates led to an autocorrelation function of the form $C(t)=2^{-t/\tau_1}$, with $\tau_1$~40 min, for both data and simulations.

**Autocorrelations in the symmetric branch experiments:** The difference between the YFP *production rate* and the CFP *production rate* was calculated at every time point for each cell, and was assigned a ranking compared to other cells at the same time point. The autocorrelation function was calculated for these rankings (Fig. 4E), yielding $\tau_{intrinsic}$<10. The same procedure was applied to the difference between *total* YFP and *total* CFP protein at each time point, with $\tau_{total}$=45±5 min. Similar results were obtained using the *ratio* of production rates (or of total proteins) rather than their differences. We obtained autocorrelation times of $\tau'_{intrinsic}$<10 min for the production rate ratios and $\tau'_{total}$=35±5 min for the total fluorescence ratios. Note that our time resolution is limited by the temporal resolution of measurements in the time-lapse experiments (<10 minutes). Folding and oxidation times of CFP and YFP were found to be < 10 minutes in *E. coli*.

**Supporting text**

**Parameters of $P_R$ promoter repression:** The dissociation constants and concentrations we obtain (Table 1) are comparable to previous estimates. *In vitro* binding assays indicate that half-maximal occupancy of the $P_R$ promoter occurs at repressor concentrations on the order of 10nM (*10-12*), although these values may be sensitive to parameters such as temperature (*11*). Total cellular λ repressor levels in lysogens have been estimated at about 140 copies of CI per cell (*13*), with measurements ranging from ~100 copies per cell (*5, 14*) to ~220 copies per cell (*15*). *In vivo* measurements indicate that half-maximal repression of the $P_R$ promoter occurs at repressor levels of roughly half that level (*8*), $k_d^{PR}$~80nM. Previous experiments suggest that half-maximal repression of the $O_R2$* mutant (designated as VN) occurs at repressor concentration ($k_d^{VN}$) which are several times higher than $k_d^{PR}$ (*3, 16*). Note that regulation of the complete $P_R$ promoter in a bacteriophage lambda lysogen may differ significantly due to other effects such as looping interactions with operator sites at $P_L$ (*8*).

**Distribution of protein production rates:** The protein production rates are distributed about the mean GRF (Fig. 3B). For each data point, with a repressor concentration $R(t)$, we divided the measured protein production rate $A(t)$ by the mean GRF value for that repressor concentration, $f(R(t))$, to obtain their ratio $\rho(t)=A(t)/f(R(t))$. The values of this ratio were distributed log-normally (Kolmogorov-Smirnov significance of 50%) rather than normally (Kolmogorov-Smirnov significance of 0.5%) and have a mean close to 1 with a standard deviation of 0.35; see Fig. S5. Similar results were obtained for the distribution of production rates $A(R_0)$ at a constant repressor concentration $R_0$. Our findings suggest that, in a single cell, whose repressor concentration is $R(t)$, the rate of production of a downstream protein corresponds to the value of the mean GRF, $f(R(t))$, modified by a noise term which is distributed log-normally (Fig. S5). This noise is not 'white', but rather has an autocorrelation time of one cell cycle (Fig. 4E). The production rate is further modified by an intrinsic noise process which has a short autocorrelation time.

**Supporting figures**

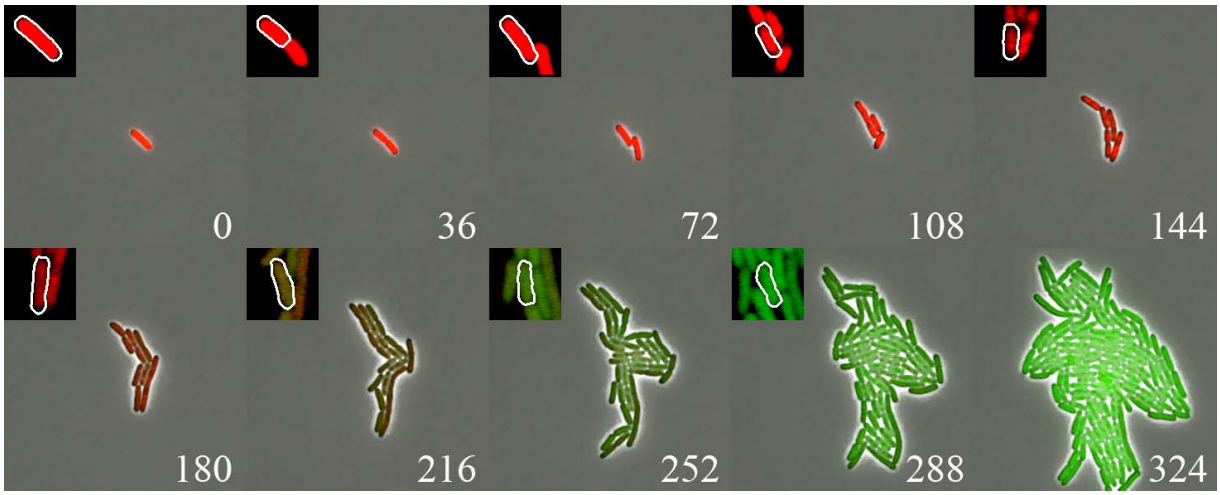


**Figure S1: Snapshots of a typical regulator dilution experiment using the $O_R2$*-λ-cascade strain**. *Panels show the same microcolony as Fig. 1D, with greater time-resolution. CI-YFP protein is shown in red and CFP is shown in green. Times, in minutes, are indicated on snapshots. Insets show a selected cell lineage (outlined in white).*

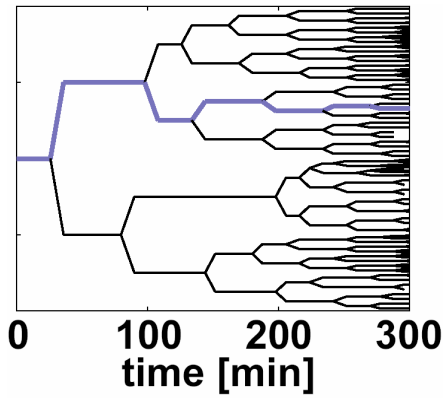


**Figure S2: Lineage tree diagram of the microcolony shown in Fig S1.** *The microcolony begins with one cell. Each splitting point corresponds to a division event, and the two sister cells branch off from the parent cell. The highlighted lineage is the one outlined in Fig. 1D, Fig. S1, and Fig. 2A.*

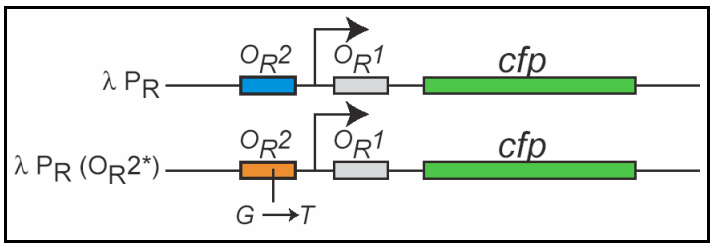


**Figure S3: Variants of the PR promoter.** *The λ-phage $P_R$ promoter contains two neighboring binding sites, $O_R1$ and $O_R2$, which allow cooperative repression (3, 5, 8, 11, 12). The $O_R2$* variant contains a single point mutation in $O_R2$ (see methods).*

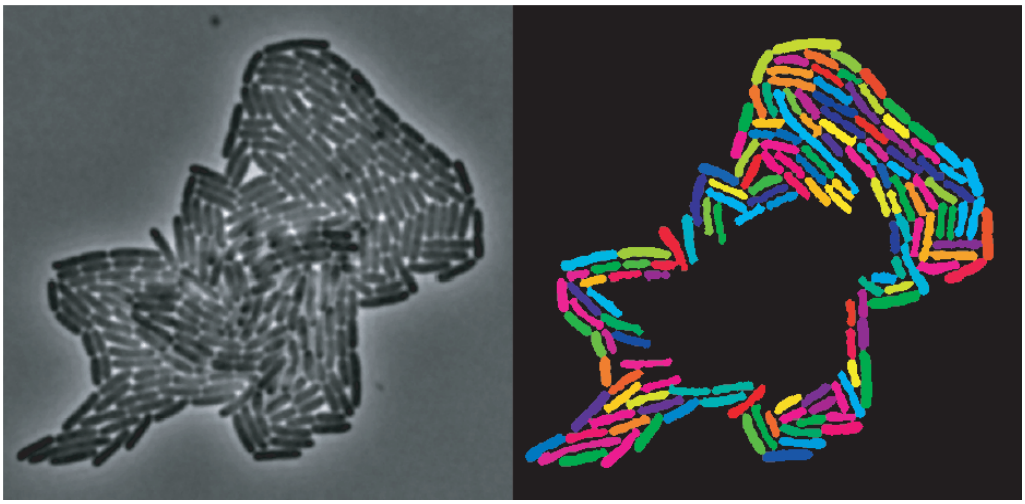

**Figure S4: Analysis of fluorescence microscopy time-lapse images.** *Phase contrast images (left) are processed with a segmentation algorithm that identifies individual cells (right). Areas where cells grow out of the focal plane (center of microcolony) are discarded. Cell coloring is arbitrary. Cell dimensions and fluorescence are measured.*

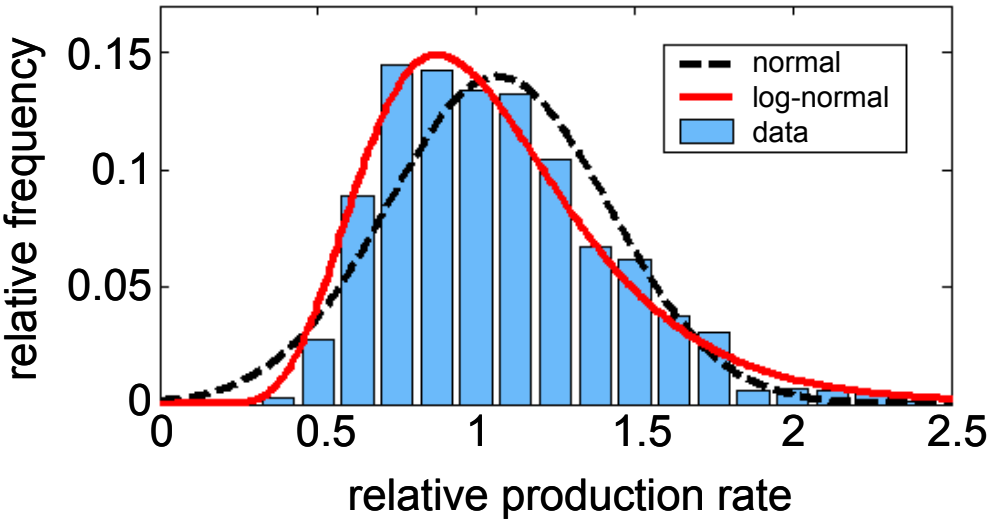


**Figure S5: Distribution of protein production rates.** *A histogram of the protein production rates of the $O_R2$* strain relative to the mean GRF (see supporting text). The log-normal distribution (solid red line) gives a better agreement with the data than the normal distribution (dashed black line).*

**Figure S6 (next page): Local micro-environment has little detectable effect on this GRF.** ***(A)*** *Three separate wild-type-λ-cascade cell lineages, with different initial repressor concentration, grow into one microcolony.* ***(B)*** *The GRFs of the three lineages have small differences compared to other sources of variation in the system. The wild-type and $O_R2$* mean GRFs are plotted as a guide to the eye (black lines).*

Figure S6

**A**

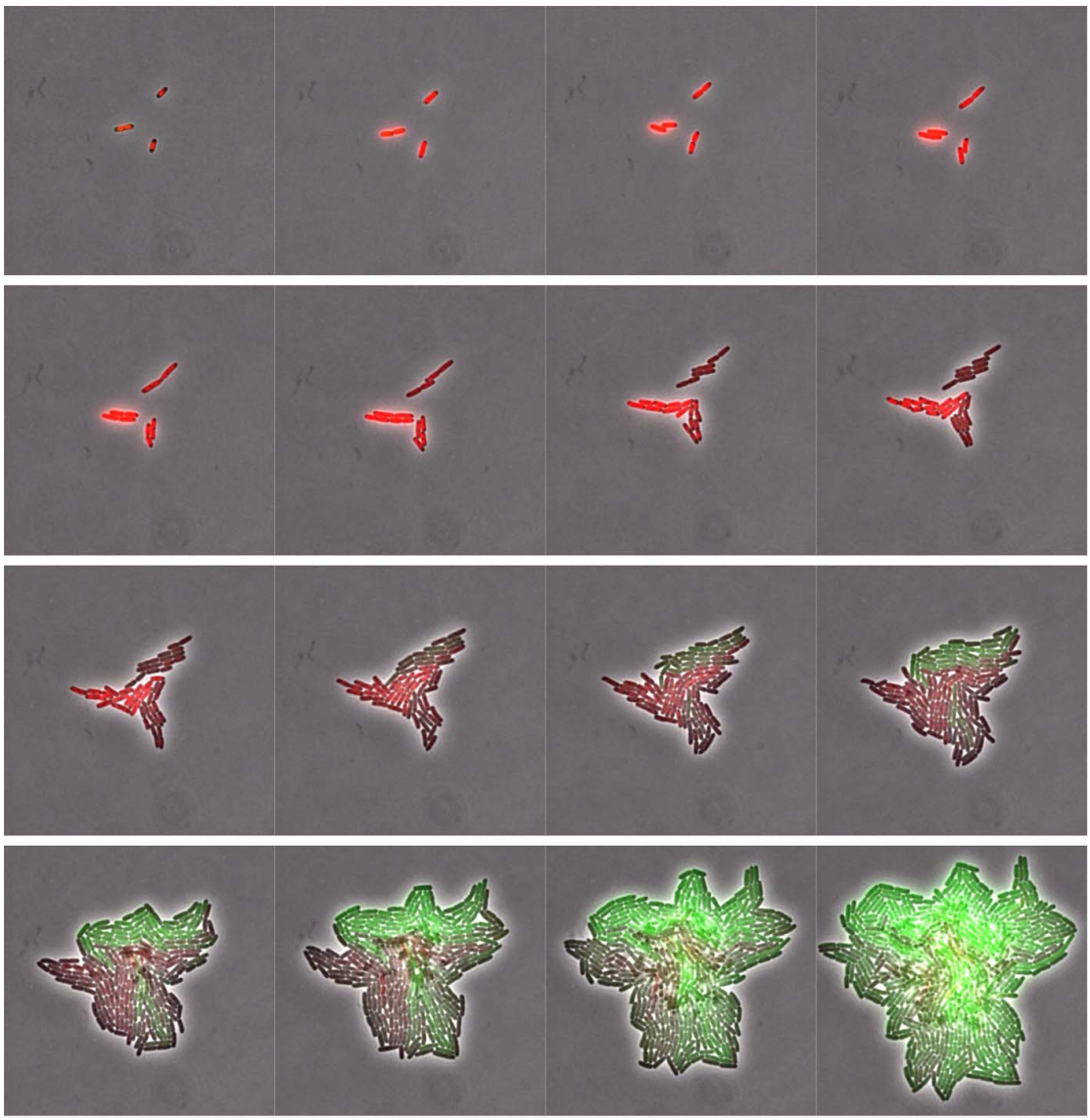

**B**

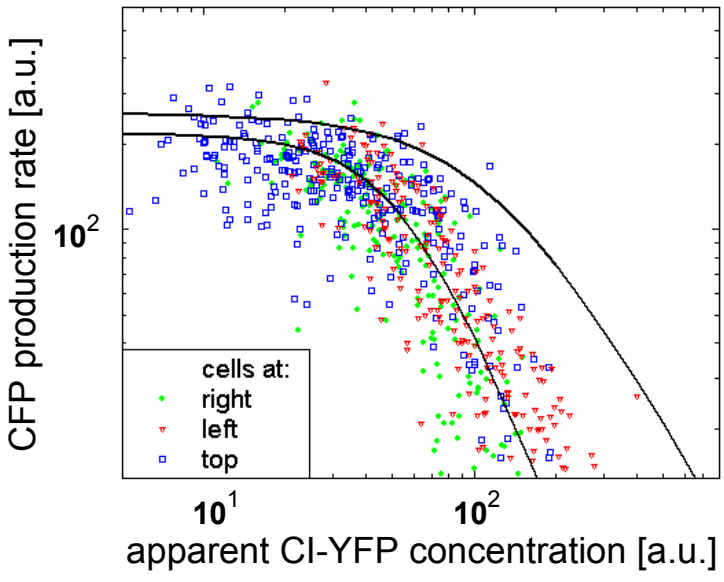
CFP production rate [a.u.]
10^2
cells at:
right
left
top
10^1
10^2
apparent CI-YFP concentration [a.u.]

**Online movies:**

**Movie S1:** *A time-lapse movie of the $O_R2$*-λ-cascade microcolony shown in Fig. 1D and in Fig. 2A. Here CI-YFP protein, shown in red, can be seen diluting out from an initial cell as it grows into a microcolony. At sufficiently low repressor levels, CFP expression, shown in green, begins. Phase contrast images are shown in the background, in gray. The time between frames in this movie is ~18 minutes. (Note that saturating color values occur during rescaling of data for display and do not indicate saturation of the original images).*

**Movie S2:** *A time-lapse movie of a wild-type-λ-cascade microcolony. Colors and the time between frames are as in movie S1.*

**Movie S3:** *A time-lapse movie of a symmetric-branch microcolony, with 9 minutes between frames. Initially, (invisible) repressor levels are high and the cell fluorescence is low. As the colony grows and the repressor is diluted, YFP (shown in red) and CFP (shown in green) both turn on, and their superposition gives a yellow color. Some cells contain relatively higher levels of CFP (green cells) and other cells contain relatively higher levels of YFP (red cells). This property has a slow drift on the order of the cell-cycle time.*

**Supporting references**


1. R. Lutz, H. Bujard, *Nucleic Acids Res* **25**, 1203-10. (1997).
2. M. B. Elowitz, A. J. Levine, E. D. Siggia, P. S. Swain, *Science* **297**, 1183-6 (Aug 16, 2002).
3. B. J. Meyer, R. Maurer, M. Ptashne, *J Mol Biol* **139**, 163-94 (May 15, 1980).
4. N. Rosenfeld, U. Alon, *J Mol Biol* **329**, 645-54 (Jun 13, 2003).
5. M. Ptashne, *A Genetic Switch* (Cell Press and Blackwell Science, ed. 2nd ed., 1992).
6. A. D. Johnson, C. O. Pabo, R. T. Sauer, *Methods Enzymol* **65**, 839-56 (1980).
7. K. S. Koblan, G. K. Ackers, *Biochemistry* **30**, 7817-21 (Aug 6, 1991).
8. I. B. Dodd *et al.*, *Genes Dev* **18**, 344-54 (Feb 1, 2004).
9. J. A. Shapiro, *Annu Rev Microbiol* **52**, 81-104 (1998).
10. A. D. Johnson, B. J. Meyer, M. Ptashne, *Proc Natl Acad Sci U S A* **76**, 5061-5 (Oct, 1979).
11. K. S. Koblan, G. K. Ackers, *Biochemistry* **31**, 57-65 (Jan 14, 1992).
12. P. J. Darling, J. M. Holt, G. K. Ackers, *J Mol Biol* **302**, 625-38 (Sep 22, 2000).
13. A. Levine, A. Bailone, R. Devoret, *J Mol Biol* **131**, 655-61 (Jul 5, 1979).
14. V. Pirrotta, P. Chadwick, M. Ptashne, *Nature* **227**, 41-4 (Jul 4, 1970).
15. L. Reichardt, A. D. Kaiser, *Proc Natl Acad Sci U S A* **68**, 2185-9 (Sep, 1971).
16. R. Maurer, B. Meyer, M. Ptashne, *J Mol Biol* **139**, 147-61 (May 15, 1980).